LANGMUIR Article
Cite This: Langmuir 2019, 35, 6922−6928
pubs.acs.org/Langmuir

Adsorptive Spin Coating To Study Thin-Film Stability in Both Wetting and Nonwetting Regimes

Yueyue Qi, Haimi Nguyen, Kelly Sin Ee Lim, Wenyun Wang, and Wei Chen*

Chemistry Department, Mount Holyoke College, South Hadley, Massachusetts 01075, United States

Supporting Information

ABSTRACT: A new thin-film fabrication method, adsorptive spin coating, was evaluated in the preparation of poly(vinyl alcohol) (PVOH) thin films on silicon-wafer-supported poly(dimethylsiloxane) (PDMS) substrates. This method takes advantage of the rapid spontaneous adsorption of PVOH at the substrate−solution interface during the brief contact period and the directionality of drying during spinning. Similar to the results obtained using dip coating, the PVOH thin films wet the 2 kDa PDMS substrate and exhibit dewetted fractal morphologies on thicker PDMS substrates. This method generated PVOH films with thicknesses that were comparable to those prepared by dip coating except that thicker PVOH films were obtained at lower spin rates, following the Meyerhofer relationship in the wetting regime. Stepwise dewetting dynamics of confined PVOH drops were captured using high-speed photography. Drying and polymer aggregation initiate at the periphery of the drop and propagate toward the center of the drop. Each dewetted thin film adopts the footprint of the original drop and shows globally ordered patterns, which depend on both initial drop size and spin rate. The PVOH thin films have excellent stability toward water rinse if they are continuous and are given sufficient time to dry. This new adsorptive spin-coating method is not only straightforward but also unique in its ability to generate globally ordered morphologies that are the outcome of fast spontaneous adsorption, spin symmetry, and temporally and spatially adjustable drying rates. It is a valuable tool for fabricating a wide range of thin-film systems where surface adsorption/reaction is rapid, in both wetting and nonwetting regimes.

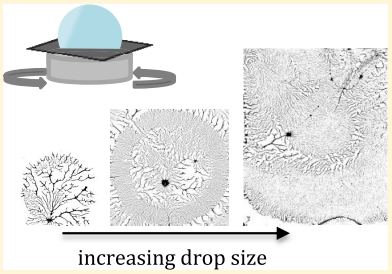

INTRODUCTION

Polymer thin films are ubiquitous in everyday life and are central to numerous industrial and biomedical applications. Typically, thin-film stability is desirable, such as in the application of coating materials. However, controlled dewetting can also be beneficial, for example, in printing and other lithographic processes. Thin-film stability has been extensively studied both experimentally and theoretically.[1−11] Mechanisms of dewetting include "spinodal dewetting" for unstable and metastable thin films below a capillary length-determined thickness, "heterogeneous nucleation" by surface defects, and "homogeneous nucleation" by thermal activation for metastable thin films.[8] The initially generated holes can continue to grow, merge, and rupture, resulting in honeycombs, ribbons, and/or droplets due to Rayleigh instabilities.[2]

Among the methods for polymer thin-film preparation, spin coating is widely used for lithography applications[12] and depositions of organic semiconductors[13,14] and polyelectrolyte layer-by-layer films.[15,16] It consists of four basic steps: deposition, spin-up, spin-off, and solvent evaporation.[17] The deposition and spin-up steps can be simultaneous or sequential with an uncontrolled amount of time in between. The setup is simple; the process is fast and reproducible. For a nonvolatile, Newtonian solution on a rotating disk, the balance between centrifugal and viscous forces results in films of uniform thickness assuming no slip at the solution−substrate interface.[18] Meyerhofer proposed a model to decouple outward flow and evaporation, allowing the prediction of film thickness (h) as a function of spin rate (w), $h = kw^{-1/2}$, where k is related to the initial solution viscosity.[19] Extrand confirmed the $-1/2$ power law for many organic polymers with thickness ranging from 0.5 to 170 nm as a function of spin rate.[20]

Although spin coating is often used for the fabrication of continuous thin films, it is also utilized in the study of thin-film instability. In the latter case, most of the systems studied involved nonpolar, nonvolatile van der Waals thin films on nonwetting solids, such as polystyrene films on silicon wafers. The stability of polymer thin films prepared from aqueous solution has not been well studied due to the additional challenge from destabilizing polar interactions during solvent evaporation.[4,6] Furthermore, even though spin-coating dynamics in the wetting regime has been studied extensively, to the best of our knowledge, dewetting dynamics has not been documented. Additionally, dewetted thin-film morphologies typically depict features on nano- to micron scales, representing areas that are orders of magnitude smaller than that of a macroscopic sample. Dewetting patterns on the entire sample are thus often left to one's speculation and imagination. A global depiction of thin-film morphology can be a useful tool in the study of drying dynamics and for the preparation of large-scale patterned surfaces.

Received: March 28, 2019
Revised: April 24, 2019
Published: May 13, 2019

DOI: 10.1021/acs.langmuir.9b00923
Langmuir 2019, 35, 6922−6928

Dip coating is another common method for thin-film preparation. It involves sample immersion in a solution of interest for a desired amount of time prior to sample removal. It does not require any special equipment and is applicable to a variety of sample shapes. The disadvantages are that it may consume a large amount of solution and often requires additional rinsing and/or drying steps.

Poly(vinyl alcohol) (PVOH) thin-film fabrication on hydrophobic substrates via dip coating was reported more than a decade ago.[21−25] The hydrophobic substrates investigated were fluoropolymers,[21−23] polyolefins,[21−23] polyesters,[21−23] polystyrene,[24] and gold.[25] PVOH is different from other water-soluble synthetic polymers, in that it is atactic yet crystalline. The driving forces for the spontaneous adsorption include hydrophobic interactions and the subsequent crystallization of PVOH polymer chains at the solid−solution interface.[22] Kinetics indicated that PVOH adsorption was fast, within minutes.[21,22] The adsorbed PVOH thin films appeared continuous by atomic force microscopy (AFM) with reproducible ellipsometric thicknesses.[22,23]

Recently, we evaluated PVOH adsorption on polydimethylsiloxane (PDMS) substrates[26,27] because of the technological importance of hydrophilizing silicones[28,29] and the unsuccessful attempts reported by others.[30−33] The PDMS substrates were prepared by the covalent attachment of linear PDMS polymers to silicon wafers.[26,34] The PDMS layer thickness varied from ∼1 to ∼11 nm as the PDMS molecular weight increased from 2 to 116 kDa. Using the dip-coating method, the PVOH film thickness was ∼3 nm, independent of the PDMS layer thickness. Different from the results obtained from the earlier studies, the PVOH morphologies progressively transitioned from continuous on PDMS^{2k} to discontinuous as PDMS thickness increased. The morphological transformation was attributed to evaporation-induced PVOH thin-film dewetting on thicker, more liquid-like PDMS layers. Interestingly, while 88%-hydrolyzed PVOH (the percentage of poly(vinyl acetate) repeat units hydrolyzed in its synthesis) films showed conventional droplet features upon dewetting, 99%-hydrolyzed PVOH films exhibited unique fractal morphologies. Polymer crystallization[22,35] in a diffusion-limited aggregation fashion[36−42] during the drying process was shown to give rise to the formation of the unusual fractal morphologies.[26] It was, however, difficult to characterize the fractal dimension (complexity)[43,44] and lacunarity (gappiness)[44,45] of the fractal morphology due to feature irregularities across sample surfaces, caused by uneven solvent evaporation during air drying. Furthermore, out of concern that some Langmuir−Blodgett-like deposition might occur when samples were removed through the solution−air interface, serial dilutions were performed prior to sample retrieval.[22,23,26] This was not only time consuming but also likely resulted in the incomplete removal of loosely attached PVOH chains from sample surfaces.

In this study, adsorptive spin coating, a hybrid between dip coating and spin coating, of PVOH solution on PDMS substrates was evaluated as a method for thin-film fabrication and stability study. A deliberate, optimized, yet short adsorption step prior to spin sets this approach apart from other thin-film fabrication techniques. This method is simple, fast, and reproducible. It provides sufficient time for the spontaneous adsorption of PVOH polymer chains to silicone substrates and allows directional drying to generate globally ordered dewetting patterns across sample surfaces.

EXPERIMENTAL SECTION

Materials. Silicon wafers (100 orientation, P/B doped, resistivity 1−10 Ω cm, thickness 475−575 μm) were purchased from International Wafer Service. Poly(vinyl alcohol) (PVOH: 89−98 kDa and >99% hydrolyzed). Trimethylsiloxy-terminated polydimethylsiloxanes (PDMS^{2k}, MW = 2 kDa; PDMS^{9k}, MW = 9 kDa; PDMS^{17k}, MW = 17 kDa; PDMS^{49k}, MW = 49 kDa; PDMS^{116k}, MW = 116 kDa) were purchased from Gelest. HPLC-grade organic solvents were obtained from Pharmco. Oxygen gas (99.999%) was purchased from Middlesex Gases Technologies. All reagents were used as received without further purification. Water was purified using a Millipore Milli-Q Biocel System (Millipore Corp., resistivity ≥18.2 MΩ/cm).

Instrumentation and Characterization. Silicon wafers were cleaned in a Harrick plasma cleaner PDC-001. Spin coating was carried out using a Laurell WS-400B-6NPP/LITE single wafer spin processor. Contact angles were measured using a Ramé−Hart telescopic goniometer with a Gilmont syringe and a 24 gauge flat-tipped needle. Dynamic advancing (θ_A) and receding (θ_R) angles were captured by a camera and digitally analyzed, while Milli-Q water in the syringe was added to and withdrawn from the drop, respectively. The standard deviation of the reported contact angle values is less than or equal to 2° unless specified otherwise. Native silicon dioxide and polymer layer thicknesses were measured using a Gaertner Scientific LSE Stokes ellipsometer at a 70° incident angle (from the normal to the plane). The light source is a He−Ne laser (λ = 632.8 nm). Thickness was calculated using the following refractive indices: air, n_o = 1; silicon oxide and polymer layers, n_1 = 1.46; silicon substrate, n_s = 3.85 and k_s = −0.02 (absorption coefficient). Measurement error is within 1 Å as specified by the manufacturer. Each of the reported thickness and contact angle value is an average of at least eight measurements obtained from at least four samples from two different batches and two readings from different locations on each sample. An Olympus BX51 optical microscope in the reflective mode was used to obtain microscopic images of substrates. Images were captured using the 1.25× and 5× objective lenses. Image merging was performed using either Autopano Giga or the Photomerge function in Photoshop to generate macroscopic images of the entire samples. Fractal dimension (D) and lacunarity (L) of fractal morphologies were determined using the Fraclac plugin in ImageJ after the images were converted to binary. The reported D and L values are averages of at least three measurements. Videos of spin-coating PVOH solutions on PDMS substrates were captured by a high-speed camera, FASTCAM SA3 model 120K-M2, at 2000 frames per second.

Preparation of PDMS Substrates.[26,34] Silicon wafers were diced into 1.2 × 1.5 or 1.4 × 1.4 cm^2 pieces, rinsed with distilled water, and dried with compressed air and in a clean oven at 110 °C for 30 min prior to being exposed to oxygen plasma at ∼300 mTorr and 30 W for 15 min. PDMS polymer (100 μL) was dispensed on each clean wafer. Samples were heated at 100 °C for 24 h in capped scintillation vials. After the reaction, the wafers were rinsed individually with toluene (3×), acetone (3×), and Milli-Q water (3×) and dried under a nitrogen stream to remove excess water and in a desiccator ($CaSO_4$) overnight.

Adsorption Kinetics of PVOH on PDMS^{2k}. A 0.1 wt% PVOH solution was prepared by dissolving 0.1 g of PVOH powder in 100 g of Milli-Q water at 88−94 °C for 3 h under stirring in a clean polypropylene bottle. The PVOH solution was used after equilibration for a few days and within 90 days of preparation. PVOH solution (3 mL) was poured into a scintillation vial containing a PDMS^{2k} sample. After a desired amount of time, ∼17 mL of Milli-Q water was added to the vial and the sample was removed immediately. The sample was rinsed with Milli-Q water (3×) and desiccated overnight.

Adsorptive Spin Coating of PVOH Solution on PDMS Substrates. A drop of PVOH solution of the desired volume was dispensed onto a PDMS substrate secured on the spin-coater stage. After 60 s, the sample was spun at the desired rate for 60 s. The sample was kept in a desiccator overnight prior to characterization.

Stability Studies. PDMS substrates coated with PVOH films were rinsed with Milli-Q water (3×, total ∼15 s), either immediately after coating or after allowing the samples to dry in a desiccator for 24 h.

DOI: 10.1021/acs.langmuir.9b00923
Langmuir 2019, 35, 6922−6928

RESULTS AND DISCUSSION

Adsorption Kinetics. An important step in establishing an appropriate protocol for adsorptive spin coating is to understand the adsorption kinetics of the system of interest. Even though PVOH adsorption kinetics on other hydrophobic substrates has been studied,[21,22] PDMS is unique so that determining adsorption kinetics is necessary. Because our earlier studies showed that the thickness of the adsorbed PVOH thin films is independent of the type of PDMS substrates, PDMS^{2k} was chosen as the substrate where continuous PVOH thin films with more reproducible thicknesses were obtained.[26] As shown in Figure 1, an equilibrium thickness of 2.5−3 nm was obtained after 10 s, the shortest time examined, indicating that the spontaneous adsorption is extremely fast. The adsorptive spin-coating method is most suitable for such a fast adsorption system where the solution concentration does not change appreciably during the adsorption period and the entire process remains expeditious. The thickness values are consistent with those from the earlier studies.[22,23,26] Due to the short adsorption times examined, the samples were removed and rinsed using a more expedited protocol (see the Experimental Section) instead of the serial dilution method. This contributes to the more pronounced thickness variations shown in Figure 1. Adsorption time of 60 s was chosen for all of the adsorptive spin-coating trials performed in this study.

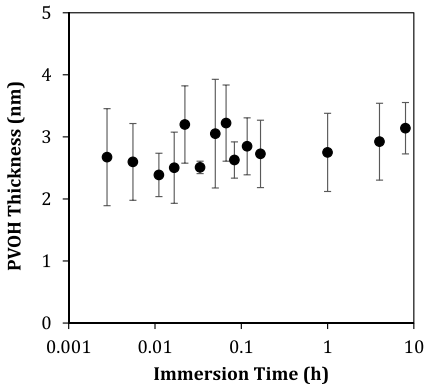

Figure 1. Adsorption kinetics of PVOH on PDMS^{2k} using dip coating.

Drying Dynamics. To understand the drying dynamics, the spin processes of a 200 μL PVOH drop on PDMS^{2k} and PDMS^{49k} substrates were captured using a high-speed camera. Movies S1 and S2 are provided in the Supporting Information. Some representative frames at 6000 rpm are shown in Figures 2 and 3. On PDMS^{2k} (Figure 2), spin initially caused the PVOH drop to elongate. Excess liquid then exited the sample, while the rest of the drop stayed pinned. These steps take place within the initial several seconds of the spin. The dried PVOH film appears smooth by both optical and AFM images. This is the wetting scenario, consistent with the findings using the dip-coating method.[26] On PDMS^{49k} (Figure 3), the process was similar to that on PDMS^{2k} except that the rest of the drop dewetted and spun-off in a stepwise fashion.

Thickness and Wettability Characterization. The thickness and dynamic water contact angles of the PVOH thin films fabricated via adsorptive spin coating were characterized. For

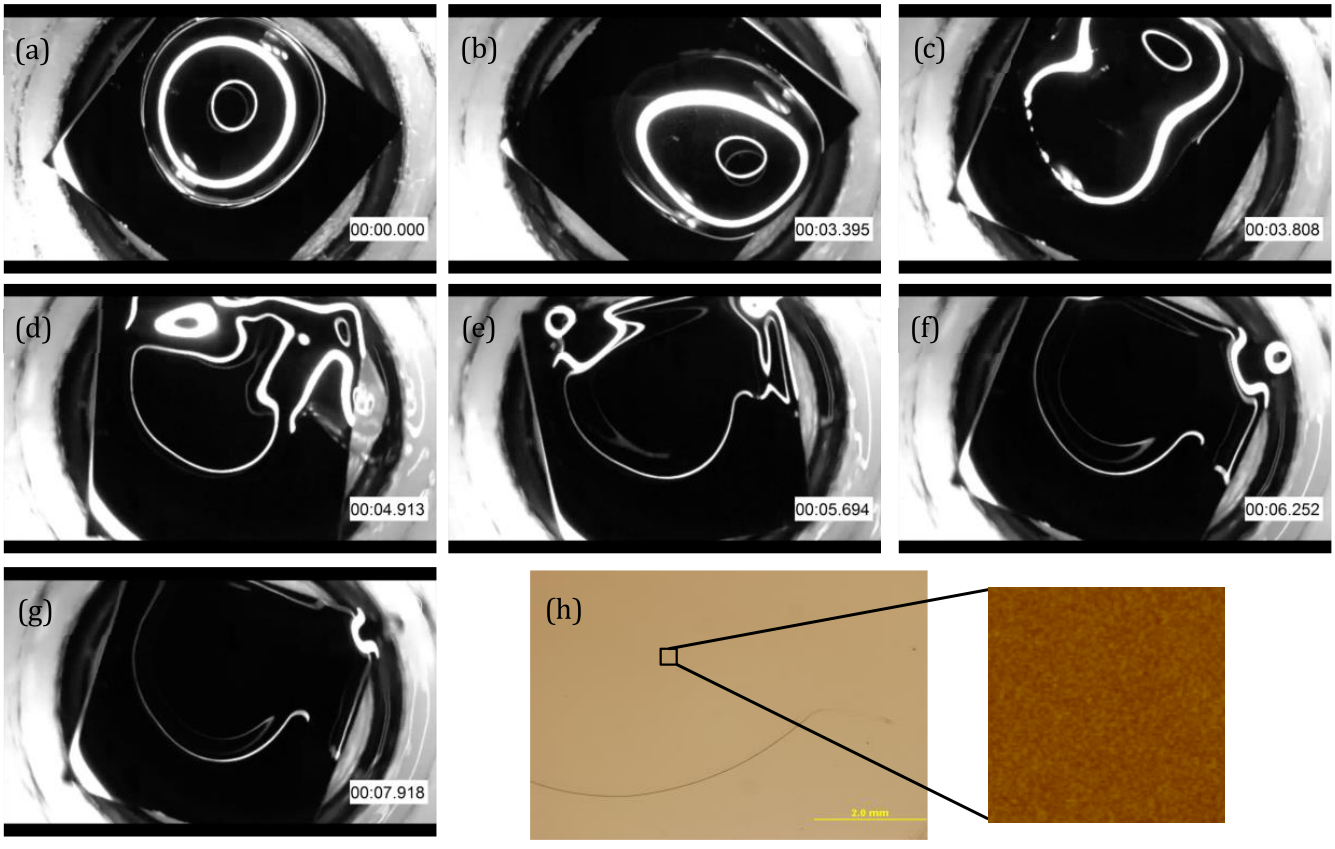

Figure 2. (a−g) Selected frames captured by a high-speed camera when 200 μL of PVOH solution was spin-coated on a 1.4 × 1.4 cm^2 silicon wafer coated with PDMS^{2k}. (h) Optical micrograph (scale bar: 2 mm) and an AFM image (size: 1 × 1 μm^2; height scale: 20 nm) of the dried drop.

DOI: 10.1021/acs.langmuir.9b00923
Langmuir 2019, 35, 6922−6928

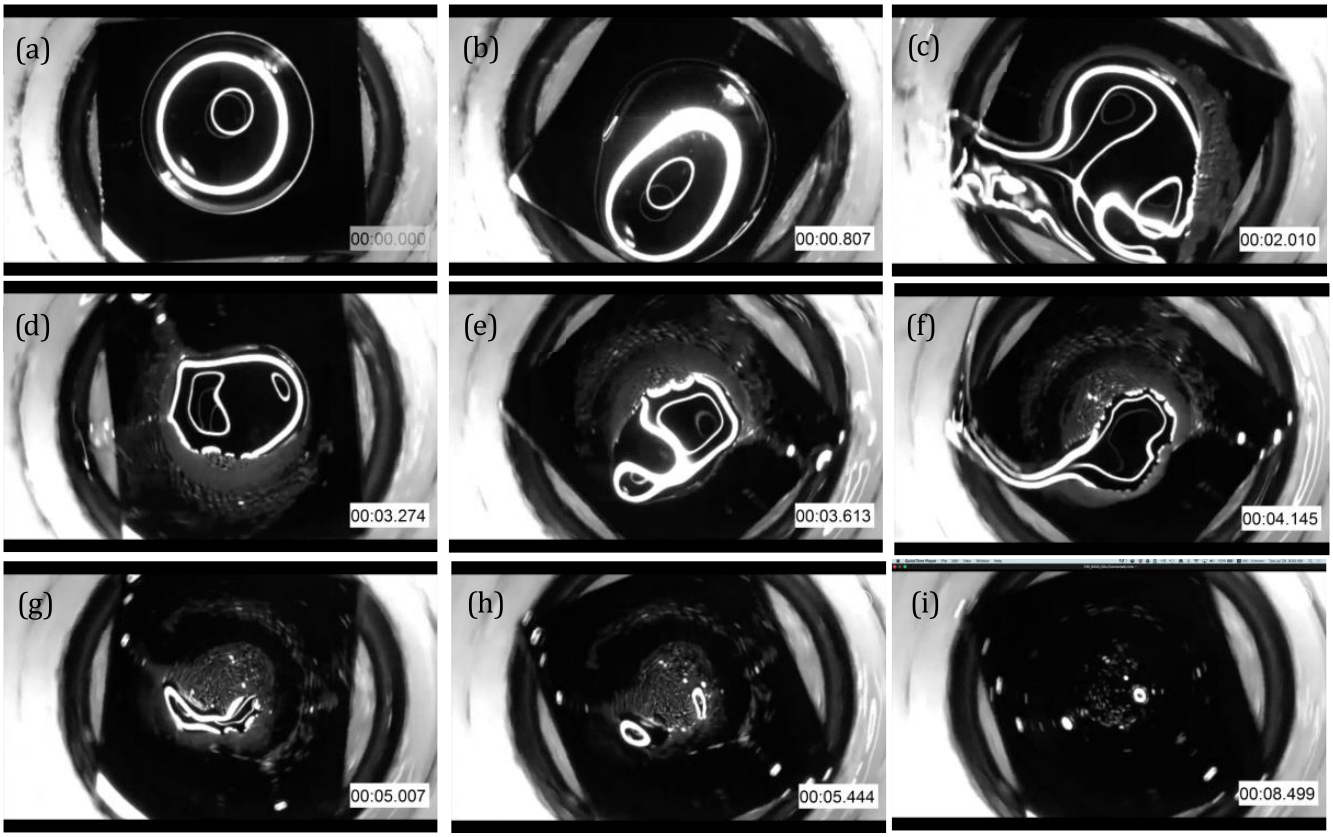

Figure 3. Selected frames captured by a high-speed camera when 200 μL of PVOH solution was spin-coated on a 1.4 × 1.4 cm^2 silicon wafer coated with PDMS^{49k}. The wafer dimension establishes the scale.

this set of experiments, the entire substrates were coated by the PVOH solution prior to spin to maximize the surface area for measurements. Film thickness on various PDMS substrates as a function of spin rate is plotted in Figure 4a. In the wetting regime on PDMS^{2k}, the PVOH film thickness exhibits a power-law relationship with the spin rate, $h \propto w^{-0.50}$, which is in excellent agreement with Meyerhofer's model.[19] However, in the dewetting regime, the average film thickness is ∼2 nm, independent of spin rate. Several conjectures can be made

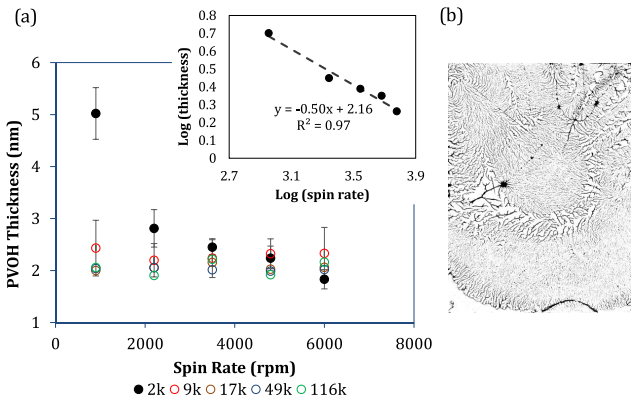

Figure 4. (a) PVOH film thickness on various PDMS substrates as a function of spin rate. The inset shows a logarithmic plot of PVOH thickness on PDMS^{2k} vs spin rate. (b) Binary optical image (1.2 cm × 1.5 cm) of a dewetted PVOH thin film prepared on PDMS^{49k} at 3500 rpm. The image was stitched together from sectional optical images (1.25×) using the Photomerge function in Photoshop.

based on these results. First of all, the Meyerhofer power law is valid only in the wetting regime because of the no-slip assumption. To the best of our knowledge, this is the first time when film thickness independent of spin rate was observed. Furthermore, the constant 2 nm film thickness in the dewetting regime corresponds to that obtained at high spin rates in the wetting regime, implying a comparable amount of PVOH adsorbed during the 60 s contact time on all PDMS substrates and that negligible additional adsorption/deposition takes place during the spin-up, spin-off, and evaporation steps under these conditions. More concentrated solutions do result in additional polymer deposition in the spin process (data not shown here). Lastly, the 2 nm thickness obtained using adsorptive spin coating is slightly less than that obtained using dip coating. The discrepancy is attributed to the differences in thin-film fabrication techniques, especially how the excess solution is removed. An optical image of a dewetted PVOH thin film on PDMS^{49k} is shown in Figure 4b. The image was constructed from many sectional images using the Photomerge function in Photoshop and provides a global depiction of a dewetted PVOH thin film. Fractal morphology is apparent and with much more order than those obtained using the dip-coating method from our previous study.[26] The film shows irregularities near the edge of the wafer and a circular pattern in the middle due to the axial symmetry of the spin process.

The advancing and receding water contact angles (θ_A/θ_R) of the substrates before and after the adsorptive spin coating of PVOH solution at 6000 rpm are shown in Table 1. The PDMS^{2k}–PVOH surface has the same contact angles as that prepared by dip coating,[26] indicating continuous coverage of the PDMS^{2k} substrate by the PVOH thin film in both cases. There is

DOI: 10.1021/acs.langmuir.9b00923
Langmuir 2019, 35, 6922−6928

Table 1. Advancing and Receding Water Contact Angles (θ_A/θ_R) of PDMS Substrates before[26] and after Spin Coating of PVOH Thin Films

θ_A/θ_R (deg)	PDMS^{2k}	PDMS^{9k}	PDMS^{17k}	PDMS^{49k}	PDMS^{116k}
before	101 ± 2/79 ± 3	107 ± 2/102 ± 2	109 ± 2/104 ± 2	109 ± 2/95 ± 2	113 ± 2/98 ± 2
after	73 ± 2/14 ± 4	108 ± 2/76 ± 8	112 ± 3/80 ± 5	113 ± 2/80 ± 4	116 ± 2/79 ± 4

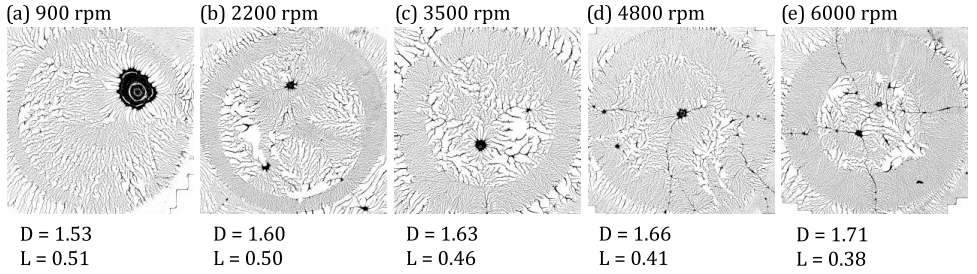

Figure 5. Binary optical images of dewetted thin films after adsorptive spin coating of a 200 μL PVOH solution (drop diameter: 9.2 ± 0.1 mm) on PDMS^{49k} at 900−6000 rpm. Each image was stitched together from sectional optical images (5×) using Autopano Giga. D and L values of the outer bands are also shown.

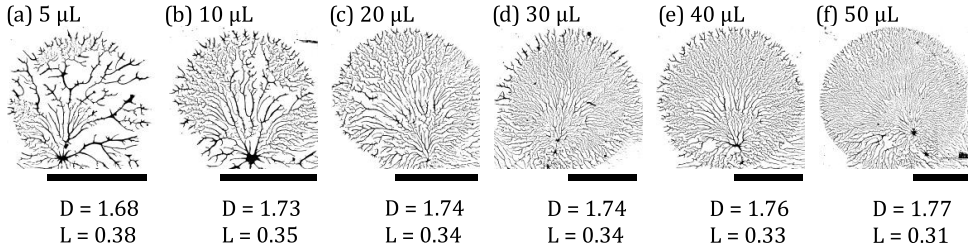

Figure 6. Binary optical images of dewetted patterns obtained from the adsorptive spin coating of a 5−50 μL PVOH solution on PDMS^{49k} at 6000 rpm. Each image was captured using the 1.25× objective lens and converted to binary after background subtraction so that D and L values could be determined. The scale bars are 2 mm in length.

a slight reduction in the receding contact angles upon PVOH adsorption on the thicker PDMS substrates due to the incomplete coverage of PDMS substrates by the PVOH thin films. The variation among the contact angle values is negligible, implying less pronounced differences in dewetted PVOH thin-film morphologies on different PDMS substrates using spin coating compared to dip coating.[21] This will be further discussed later. The standard deviations of the receding contact angles on dewetted PVOH films are high, reflecting the heterogeneous nature of the fractal morphologies.

Dewetted Patterns. To remove the edge effect observed in Figure 4b, confined PVOH drops of 200 μL in volume were cast on PDMS substrates. The optical images of the dewetted PVOH films on PDMS^{49k} at different spin rates are shown in Figure 5. The features outside the circular footprints of the original drops are caused by the spin-off of the excess solution. Considering the minimal contact time between the PVOH solution and the exit region, polymer adsorption is apparently fast enough to leave dewetted patterns behind. The features within the drop region consist of an ordered, dense outer band and a less ordered, loose inner core. The layered structure results from the stepwise dewetting process shown in Figure 3. This is consistent with the fact that centrifugal force and drying time are radially dependent. As spin rate increases, the outer band appears thicker, denser, and more homogeneous. The fractal dimension (D) and lacunarity (L) values determined using the Fraclac plugin in ImageJ are consistent with the qualitative observations of density and homogeneity. These trends result from the larger centrifugal force, faster drying rate, and shorter time for polymer chains to diffuse, aggregate, and crystallize at higher spin rates. The core region consists of larger and less ordered fractal features due to the slower drying rate and longer time for polymer thin films to dewet. The dark spots are where the last droplet(s) resided (see the two droplets in Figure 3h,i). The "veins" originating from the dark spots correspond to the secondary spin-off paths of excess solution (see Figure 3f). Similar layered structures of dewetted PVOH patterns were obtained when PDMS thickness increases from PDMS^{9k} to PDMS^{49k}, as shown in Figure S3 in the Supporting Information. In the outer band region, slightly larger and coarser fractal features were obtained on thicker, more liquid-like PDMS layers. This trend is consistent with that observed using the dip-coating method although it is not nearly as pronounced due to the shorter drying (dewetting) time. The less marked effect of PDMS layer thickness on dewetted PVOH thin-film morphology is consistent with the similarities among the dynamic water contact angles on these samples shown in Table 1.

To reduce the complexity of the layered features, smaller drops of 5−50 μL were evaluated on PDMS^{49k}. The optical images of the dewetted PVOH films are shown in Figure 6. With the smaller drops, the outer bands are absent, indicating that dewetting is close to a concerted one-step process. The fractal morphologies in the footprint of the original PVOH drop show circular symmetry and are more ordered and pronounced. The features from the smaller drops are visually coarser and more open than those from the larger drops, which is confirmed by the D and L values. This is because the smaller drops take longer to dry and so the polymer chains in the smaller drops have more time to diffuse, aggregate, and crystallize. It is interesting to note that there are fewer but larger "nucleation" sites at the periphery

DOI: 10.1021/acs.langmuir.9b00923
Langmuir 2019, 35, 6922−6928

of the smaller drops. The spin dynamics results in the initiation of the fractal feature formation at the edge and the propagation toward the middle of the drop. It should be noted that the fractal features converge at an off-center point in the spin-off direction.

Drying is fast using spin coating relative to other common coating methods. The resulting film morphologies shown in Figures 5 and 6 are thus arguably in kinetically trapped states. As discussed earlier, drying time depends on the radial distance from the spin axis and spin rate. Since the amount of polymer adsorbed per unit area is the same, the diversity among the various dewetted morphologies can be attributed solely to the different extent of polymer diffusion and aggregation during the drying step. The rapid spontaneous adsorption, the temporal and spatial dependences of the dewetting characteristics, and the axis symmetry of the spin process give rise to the unique and globally ordered morphologies. The adsorptive spin-coating method allows easy access to these interesting states.

Stability of PVOH Films. The stability of the prepared PVOH thin films was evaluated by rinsing in water to remove loosely attached polymer chains, either immediately after spin coating or after 24 h drying in a desiccator. The PVOH film thickness on $PDMS^{2k}$ and $PDMS^{49k}$ before and after rinsing is shown in Figure 7. The continuous PVOH thin films on $PDMS^{2k}$

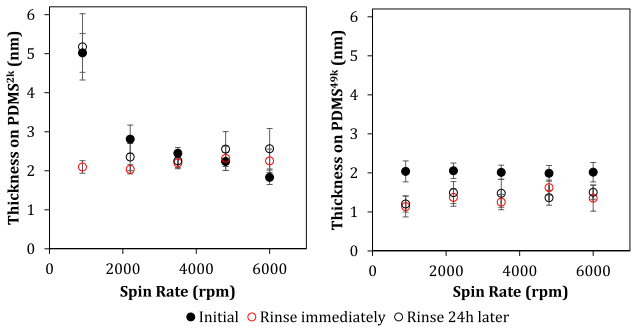

Figure 7. Thickness of PVOH films spin-coated on $PDMS^{2k}$ (left) and $PDMS^{49k}$ (right) at 6000 rpm: initial (filled black circles) and after rinsing (open black circles for rinsing immediately and open red circles for rinsing after 24 h).

after 24 h drying are completely stable so that negligible thickness changes within standard deviations were observed. However, if rinsed immediately, thicknesses decreased to a constant value of ~2 nm, which is the same as the thickness value obtained in the dewetting regime and at high spin rates in the wetting regime. We hypothesize that the total PVOH thickness in the wetting regime consists of ~2 nm from spontaneous adsorption and additional polymer deposition from solvent evaporation during the later stage of spin coating. Our earlier work showed that the spontaneously adsorbed, 99%-hydrolyzed PVOH thin films are crystalline in nature.[26] The additionally deposited portion appears to be largely amorphous and unstable toward water rinse unless it is given time to dry and crystallize. The results are different for dewetted PVOH thin films on $PDMS^{49k}$. Significant film loss was observed after either rinsing protocol. The high surface area renders the amorphous portion of the dewetted thin films more susceptible to dissolution in water. The drying step does not noticeably enhance the stability of the dewetted thin films. More work is underway to study the effects of crystallization and surface area on the stability of the PVOH thin films prepared using adsorptive spin coating.

SUMMARY AND CONCLUSIONS

In this research, a new adsorptive spin-coating method, taking advantage of spontaneous adsorption and directional spin coating, was evaluated for fabricating PVOH thin films on PDMS substrates. Comparing the results from this method to those obtained from the dip-coating method, the wetting and dewetting behaviors of PVOH thin films on various PDMS substrates are the same. The PVOH film thickness values are similar as well, except thicker films can also be obtained at lower spin rates following the Meyerhofer relationship in the wetting regime. Dewetting dynamics of confined PVOH drops during spin were revealed by high-speed videos. Drying, polymer aggregation, and crystallization initiate at the periphery of the drop and propagate toward the center, in a stepwise fashion for large drops. Each PVOH thin film prepared by the adsorptive spin-coating method consists of a spontaneously adsorbed layer and an additionally deposited portion during the spin process. Both surface area and extent of drying or crystallization ultimately affect the stability of the PVOH thin films. In summary, the adsorptive spin-coating method is capable of generating globally ordered fractal morphologies that are the outcome of fast spontaneous adsorption, spin symmetry, and temporally and spatially adjustable drying rates. This provides access to various kinetically trapped morphological states that are critical in the study of thin-film stability. It is equally important that this method can be applied toward fabricating other thin-film systems where solute molecules, such as proteins, polyelectrolytes, and polyphenols, rapidly adhere to substrates via various types of interactions.

ASSOCIATED CONTENT

Supporting Information

The Supporting Information is available free of charge on the ACS Publications website at DOI: 10.1021/acs.langmuir.9b00923.

Movies of spin dynamics of PVOH drops on different PDMS substrates (MOV) (MOV)

Optical images of dewetted PVOH drops on different PDMS substrates (PDF)

AUTHOR INFORMATION

Corresponding Author

*E-mail: weichen@mtholyoke.edu. Phone: 413-538-2224. Fax: 413-538-2327.

ORCID

Wei Chen: 0000-0002-6970-3455

Notes

The authors declare no competing financial interest.

ACKNOWLEDGMENTS

Financial support was provided by the National Science Foundation (DMR-1404668 and DMR-1807186) and Mount Holyoke College. The authors are grateful to Professor Al Crosby and his group for their assistance with capturing the high-speed videos and to Jerry Xu for his help in processing the videos.

REFERENCES

(1) Vrij, A. Possible Mechanism for the Spontaneous Rupture of Thin, Free Liquid Films. *Discuss. Faraday Soc.* **1966**, *42*, 23−33.

DOI: 10.1021/acs.langmuir.9b00923
Langmuir 2019, 35, 6922−6928

(2) Reiter, G. Dewetting of Thin Polymer Films. *Phys. Rev. Lett.* **1992**, *68*, 75−78.
(3) Reiter, G. Unstable Thin Polymer Films: Rupture and Dewetting Processes. *Langmuir* **1993**, *9*, 1344−1351.
(4) Sharma, A. Relationship of Thin Film Stability and Morphology to Macroscopic Parameters of Wetting in the Apolar and Polar Systems. *Langmuir* **1993**, *9*, 861−869.
(5) Stange, T. G.; Evans, D. F.; Hendrickson, W. A. Nucleation and Growth of Defects Leading to Dewetting of Thin Polymer Films. *Langmuir* **1997**, *13*, 4459−4465.
(6) Thiele, U.; Mertig, M.; Pompe, W. Dewetting of An Evaporating Thin Liquid Film: Heterogeneous Nucleation and Surface Instability. *Phys. Rev. Lett.* **1998**, *80*, 2869−2872.
(7) Xie, R.; Karim, A.; Douglas, J. F.; Han, C. C.; Weiss, R. A. Spinodal Dewetting of Thin Polymer Films. *Phys. Rev. Lett.* **1998**, *81*, 1251−1254.
(8) Seemann, R.; Herminghaus, S.; Jacobs, K. Dewetting Patterns and Molecular Forces: a Reconciliation. *Phys. Rev. Lett.* **2001**, *86*, 5534−5537.
(9) Gentili, D.; Foschi, G.; Valle, F.; Cavallini, M.; Biscarini, F. Applications of Dewetting in Micro and Nanotechnology. *Chem. Soc. Rev.* **2012**, *41*, 4430−14.
(10) Xue, L.; Han, Y. Pattern Formation by Dewetting of Polymer Thin Film. *Prog. Polym. Sci.* **2011**, *36*, 269−293.
(11) Mukherjee, R.; Sharma, A. Instability, Self-Organization and Pattern Formation in Thin Soft Films. *Soft Matter* **2015**, *11*, 8717−8740.
(12) Grigorescu, A. E.; Hagen, C. W. Resists for Sub-20-Nm Electron Beam Lithography with a Focus on HSQ: State of the Art. *Nanotechnology* **2009**, *20*, No. 292001.
(13) Zhang, F.; Di, C.-A.; Berdunov, N.; Hu, Y.; Hu, Y.; Gao, X.; Meng, Q.; Sirringhaus, H.; Zhu, D. Ultrathin Film Organic Transistors: Precise Control of Semiconductor Thickness via Spin-Coating. *Adv. Mater.* **2013**, *25*, 1401−1407.
(14) Yuan, Y.; Giri, G.; Ayzner, A. L.; Zoombelt, A. P.; Mannsfeld, S. C. B.; Chen, J.; Nordlund, D.; Toney, M. F.; Huang, J.; Bao, Z. Ultra-High Mobility Transparent Organic Thin Film Transistors Grown by an Off-Centre Spin-Coating Method. *Nat. Commun.* **2014**, *5*, No. 3327.
(15) Cho, J.; Char, K.; Hong, J.-D.; Lee, K.-B. Fabrication of Highly Ordered Multilayer Films Using a Spin Self-Assembly Method. *Adv. Mater.* **2001**, *13*, 1076−1078.
(16) Chiarelli, P. A.; Johal, M. S.; Casson, J. L.; Roberts, J. B.; Robinson, J. M.; Wang, H.-L. Controlled Fabrication of Polyelectrolyte Multilayer Thin Films Using Spin-Assembly. *Adv. Mater.* **2001**, *13*, 1167−1171.
(17) Bornside, D. E.; Macosko, C. W.; Scriven, L. E. On the Modeling of Spin. *Coating. J. Imaging Technol.* **1987**, *13*, 122−130.
(18) Emslie, A. G.; Bonner, F. T.; Peck, L. G. Flow of a Viscous Liquid on a Rotating Disk. *J. Appl. Phys.* **1958**, *29*, 858−862.
(19) Meyerhofer, D. Characteristics of Resist Films Produced by Spinning. *J. Appl. Phys.* **1978**, *49*, 3993−3997.
(20) Extrand, C. W. Spin Coating of Very Thin Polymer Films. *Polym. Eng. Sci.* **1994**, *34*, 390−394.
(21) Coupe, B.; Chen, W. A New Approach to Surface Functionalization of Fluoropolymers. *Macromolecules* **2001**, *34*, 1533−1535.
(22) Kozlov, M.; Quarmyne, M.; Chen, W.; McCarthy, T. J. Adsorption of Poly(vinyl alcohol) onto Hydrophobic Substrates. A General Approach for Hydrophilizing and Chemically Activating Surfaces. *Macromolecules* **2003**, *36*, 6054−6059.
(23) Kozlov, M.; McCarthy, T. J. Adsorption of Poly(vinyl alcohol) From Water to A Hydrophobic Surface: Effects of Molecular Weight, Degree of Hydrolysis, Salt, and Temperature. *Langmuir* **2004**, *20*, 9170−9176.
(24) Barrett, D. A.; Hartshorne, M. S.; Hussain, M. A.; Shaw, P. N.; Davies, M. C. Resistance to Nonspecific Protein Adsorption by Poly(vinyl alcohol) Thin Films Adsorbed to A Poly(styrene) Support Matrix Studied Using Surface Plasmon Resonance. *Anal. Chem.* **2001**, *73*, 5232−5239.
(25) Serizawa, T.; Hashiguchi, S.; Akashi, M. Stepwise Assembly of Ultrathin Poly(vinyl alcohol) Films on A Gold Substrate by Repetitive Adsorption/Drying Processes. *Langmuir* **1999**, *15*, 5363−5368.
(26) Karki, A.; Nguyen, L.; Sharma, B.; Yan, Y.; Chen, W. Unusual Morphologies of Poly(vinyl alcohol) Thin Films Adsorbed on Poly(dimethylsiloxane) Substrates. *Langmuir* **2016**, *32*, 3191−3198.
(27) Yan, Y.; Qi, Y.; Chen, W. Strategies to Hydrophilize Silicones via Spontaneous Adsorption of Poly(vinyl alcohol) From Aqueous Solution. *Colloids Surf., A* **2018**, *546*, 186−193.
(28) Zhou, J.; Ellis, A. V.; Voelcker, N. H. Recent Developments in PDMS Surface Modification for Microfluidic Devices. *Electrophoresis* **2010**, *31*, 2−16.
(29) Zhou, J.; Khodakov, D. A.; Ellis, A. V.; Voelcker, N. H. Surface Modification for PDMS-Based Microfluidic Devices. *Electrophoresis* **2012**, *33*, 89−104.
(30) Wu, D.; Luo, Y.; Zhou, X.; Dai, Z.; Lin, B. Multilayer Poly(vinyl alcohol)-Adsorbed Coating on Poly(dimethylsiloxane) Microfluidic Chips for Biopolymer Separation. *Electrophoresis* **2005**, *26*, 211−218.
(31) Carneiro, L. B.; Ferreira, J.; Santos, M. J. L.; Monteiro, J. P.; Girotto, E. M. A New Approach to Immobilize Poly(vinyl alcohol) on Poly(dimethylsiloxane) Resulting in Low Protein Adsorption. *Appl. Surf. Sci.* **2011**, *257*, 10514−10519.
(32) He, T.; Liang, Q.; Zhang, K.; Mu, X.; Luo, T.; Wang, Y.; Luo, G. A Modified Microfluidic Chip for Fabrication of Paclitaxel-Loaded Poly(L-Lactic Acid) Microspheres. *Microfluid. Nanofluid.* **2011**, *10*, 1289−1298.
(33) Yu, L.; Li, C. M.; Zhou, Q.; Luong, J. H. T. Poly(vinyl alcohol) Functionalized Poly(dimethylsiloxane) Solid Surface for Immunoassay. *Bioconjugate Chem.* **2007**, *18*, 281−284.
(34) Krumpfer, J. W.; McCarthy, T. J. Rediscovering Silicones: "Unreactive" Silicones React with Inorganic Surfaces. *Langmuir* **2011**, *27*, 11514−11519.
(35) Bunn, C. W. Crystal Structure of Polyvinyl Alcohol. *Nature* **1948**, *161*, 929−930.
(36) Witten, T. A.; Sander, L. M. Diffusion-Limited Aggregation, A Kinetic Critical Phenomenon. *Phys. Rev. Lett.* **1981**, *47*, 1400−1403.
(37) Witten, T. A.; Sander, L. M. Diffusion-Limited Aggregation. *Phys. Rev. B* **1983**, *27*, 5686−5697.
(38) Meakin, P. Diffusion-Controlled Cluster Formation in Two, Three, and Four Dimensions. *Phys. Rev. A* **1983**, *27*, 604−607.
(39) Chen, L.; Xu, J.; Fleming, P.; Holmes, J. D.; Morris, M. A. Dynamic Stable Nanostructured Metal Oxide Fractal Films Grown on Flat Substrates. *J. Phys. Chem. C* **2008**, *112*, 14286−14291.
(40) Haberko, J.; Bernasik, A.; Łużny, W.; Raczkowska, J.; Rysz, J.; Budkowski, A. Dendrites and Pillars in Spin Cast Blends of Polyaniline or Its Oligomeric Analogue. *Synth. Met.* **2010**, *160*, 2459−2466.
(41) Samanta, T.; Mukherjee, M. Effect of Added Salt on Morphology of Ultrathin Polyelectrolyte Films. *Polymer* **2012**, *53*, 5393−5403.
(42) Zhai, X.; Wang, W.; Zhang, G.; He, B. Crystal Pattern Formation and Transitions of PEO Monolayers on Solid Substrates From Nonequilibrium to Near Equilibrium. *Macromolecules* **2006**, *39*, 324−329.
(43) Nadal, J. P.; Derrida, B.; Vannimenus, J. Directed Diffusion-Controlled Aggregation Versus Directed Animals. *Phys. Rev. B* **1984**, *30*, 376−383.
(44) Smith, T. G., Jr.; Lange, G. D.; Marks, W. B. Fractal Methods and Results in Cellular Morphology - Dimensions, Lacunarity and Multifractals. *J. Neurosci. Methods* **1996**, *69*, 123−136.
(45) Plotnick, R. E.; Gardner, R. H.; Hargrove, W. W.; Prestegaard, K.; Perlmutter, M. Lacunarity Analysis: A General Technique for the Analysis of Spatial Patterns. *Phys. Rev. E* **1996**, *53*, 5461−5468.

DOI: 10.1021/acs.langmuir.9b00923
Langmuir 2019, 35, 6922−6928